Velocity Field of an Axisymmetric Pulsed, Subsonic Air Jet

Klaus Bremhorst* and Peter G. Hollis†
University of Queensland, St. Lucia 4072, Australia

Laser Doppler anemometer measurements in a fully pulsed, subsonic air jet with a significant no-flow period between pulses have been conducted and show much higher entrainment than steady or partially pulsed jets of the same mass flow. The mean centerline velocity decay is linearly related to the inverse of the effective distance from exit for some 50 diameters, but centerline velocity decay is much slower than for steady jets due to domination by the periodic component and its associated pressure field, which affects jet momentum. For larger distances, the decay changes to the steady jet rate. Reynolds stresses are considerably larger than for a steady jet and are considered to be responsible for the increased entrainment. Results are, except for a small increase in the constant of proportionality, consistent with Taylor's entrainment hypothesis. Phase averaged results through a cycle show the ratio of shear stress to turbulent kinetic energy to be in the range of 0.2–0.3 for the bulk of the flow.

Introduction

VELOCITY field structure of steady jets has been explored extensively in the last few decades. Such studies have also led to an interest in partially pulsed or periodically perturbed jets. Studies by Crow and Champagne[1] observed an increase in entrainment of ambient fluid when a small periodic pulsation was introduced into the jet. Binder et al.[2] showed that entrainment increased with increasing level of pulsation and that the spread of the jet was dependent on both the level and frequency of pulsation.

Higher levels of entrainment are of interest for any mixing operation where the length of the mixing zone must be kept at a minimum. Applications can be found in VTOL/STOL thrusters, jet-type burners requiring external mixing with oxidizers, product mixing in the chemical industry, and dispersal of exhaust gases. An example of thrust augmentation by use of nonsteady jets can be found in Sarohia et al.[3] and Bernal and Sarohia[4] for pulsation amplitudes up to 17% of the mean velocity. A better knowledge of the velocity field of such jets is also required for the development of theories for the prediction of noise from pulsed exhausts of pneumatic drills in the mining and civil engineering industries.

As pointed out by McCroskey,[5] few analyses appear to be available for pulsed jets, a situation that is still applicable, particularly for fully pulsed jets where flow velocity is reduced to zero at the end of each pulsing cycle. In order to categorize pulsed jets, reference can be made to the Navier-Stokes equations. Thus, jets can be considered according to the significance of local acceleration to convective acceleration and pressure variation relative to stream momentum. Local acceleration is negligible when the product of amplitude ratio and Strouhal number is much less than unity and pressure effects are negligible for lightly pulsed or perturbed jets. Transition from one type of jet to the other is not well documented and little data appear to be available to provide an insight into pressure effects. Addition of a significant nonflow period between flow pulses also has not yet been investigated.

Received July 17, 1989; revision received Jan. 2, 1990.

*Associate Professor, Department of Mechanical Engineering.
†Postdoctoral Research Fellow, Department of Mechanical Engineering.

An attempt to provide some basic information for fully pulsed jets with a considerable no-flow period between pulses was made by Bremhorst and Harch[6] using hot-wire anemometer techniques. These results were placed in perspective relative to many other nonsteady jets by Bremhorst[7] and Platzer et al.[8] and extended to pulsed core jets by Bremhorst and Watson.[9] A comparison of centerline velocity decay for the various unsteady jets showed no clear pattern. Even though in all cases only convective acceleration dominated and no pressure effects were reported, few showed a trend toward steady jet behavior after the adjustment region immediately downstream of the exit. This would indicate that either the adjustment to eventual steady jet behavior is very slow or a totally different jet develops as a result of the changed initial conditions. The latter appears unlikely if the lightly perturbed results of Crow and Champagne[1] are considered for which steady jet decay is approached after only 10 exit diameters downstream. Unfortunately, the results of Binder et al.[2] contradict this for a jet of similar ratio of local to convective acceleration. Similar uncertainties exist with the rate of spread of the jet as judged by the half value radius as a function of distance from jet exit.[7] The limited, fully pulsed jet results by Bremhorst and Harch[6] show even greater differences in behavior, with the centerline velocity decay being much less than for steady and lightly pulsed jets. The preceding data do, however, show that pulsed and, especially, fully pulsed jets have significant increases in entrainment for a given length of jet, thus making them of considerable practical interest.

A more fundamental view of nonsteady jet behavior was taken by Kato et al.,[10] who postulated that entrainment velocity is a function of not just a local velocity scale, such as the jet centerline velocity, but also its time derivative. Such an hypothesis is an extension of the original Taylor entrainment hypothesis,[11] which states that the "mean inflow velocity across the edge of a turbulent flow is assumed to be proportional to a characteristic velocity, usually the local time-averaged maximum mean velocity or the mean velocity over the cross-section at the level of inflow." Telford,[12] on the other hand, takes the view that mixing, and, hence, entrainment, is a function of turbulence level. This would, in turn, relate entrainment to Reynolds stress.

The aim of the work reported here is to determine the velocity field of a fully pulsed, axisymmetric air jet. The new results together with application of the Reynolds form of the Navier-Stokes equations are then used to give a coherent and physically based explanation for the significantly changed characteristics of this type of jet.

Terminology and Definitions

Velocity and pressure are considered to consist of mean, periodic, and intrinsic turbulence components. Ensemble averaging over many cycles will yield a periodic signal, the value of which at a given instant τ_P in the pulse relative to its start is U_P, as defined by Eq. (1) for the streamwise velocity,

$$U_P = \lim_{N\to\infty} \frac{1}{N} \sum_{n=1}^{N} U_{i,\tau_P,n} \tag{1}$$

where N is the number of pulses and $U_{i,\tau_P,n}$ is the instantaneous velocity U_i at time τ_P for the nth pulse. Time averaging of the periodic component over one full cycle yields the mean value. Averaging of the instantaneous signal over a sufficiently long time also yields the mean value.

Total or aggregrate turbulence u is defined as $(U_i - U)$, but turbulence defined relative to the periodic velocity is designated as intrinsic turbulence u_I or random turbulence. If an overbar denotes time averaging, then, for the streamwise velocity, $\bar{u}_I = \bar{u}_P = \bar{u} = 0$. Similar definitions apply to velocities in the radial and azimuthal directions. Valve opening and start of pulse are assumed to coincide or differ by a fixed delay period.

Basic Equations

The Reynolds form of the axial Navier-Stokes equation for a steady, incompressible, axisymmetric flow without swirl and negligible molecular effects is

$$U\frac{\partial U}{\partial x} + V\frac{\partial U}{\partial r} = -\frac{1}{\rho}\frac{\partial P}{\partial x} - \frac{\partial \overline{u^2}}{\partial x} - \frac{\partial \overline{ruw}}{r\partial r} \tag{2}$$

Integration across the jet leads to the pressure-momentum conservation result of Eq. (3), where the first two components represent the total axial momentum in Eq. (4):

$$\frac{\partial}{\partial x}\int_0^\infty \left(U^2 + \overline{u^2} + \frac{P}{\rho}\right) r\,dr = 0 \tag{3}$$

$$\frac{\text{jet momentum}}{2\pi\rho} = \int_0^\infty (U^2 + \overline{u^2}) r\,dr \tag{4}$$

Grinstein et al.[13] studied axial momentum development of a steady jet. In the region from nozzle exit to five exit diameters downstream, a significant increase in the axial momentum represented by the first two terms of Eq. (3) was noted. For a high velocity, in steady jets as well as perturbed jets, momentum increases in this region of up to 9% were calculated. These momentum increases were found to be equal and opposite to the decrease in static pressure, thus giving the necessary conservation of momentum embodied in the Navier-Stokes equations.

Further downstream, the pressure gradient and axial gradient of $\overline{u^2}$ in Eq. (2) can be neglected for steady and lightly pulsed jets. In the case of a strongly or fully pulsed jet, neither of these simplifications necessarily follow. Upon valve opening, a pressure wave travels from the valve at sonic velocity, but if the mass of air in a pulse is small relative to the mass of air in the plenum chamber, plenum pressure will remain essentially constant and above ambient. Therefore, flow will take place in a varying pressure field resulting in flow acceleration and, hence, momentum increase. Furthermore, the large pulsations can be expected to increase the significance of the axial gradient of u^2.

Experimental Equipment and Instrumentation

The jet facility consisted of a plenum chamber with a free internal space of 260 mm in diameter and 720 mm long. A rounded, smooth transition piece connected the plenum vessel to the valve, the exit of which was fitted with a contraction to a 25.4-mm diam to give an axisymmetric jet[6] (see Fig. 1). Valve geometry resulted in an on-to-off ratio of 1 : 2. All results reported were obtained at a pulsation frequency of 10 Hz and mean velocity $\bar{U}$ of 36.6 ms^{-1} for which the mean plenum gauge pressure was 30 kPa. The corresponding Reynolds number based on exit diameter is 6.0×10^4, whereas the Strouhal number based on mean velocity is 0.007. The resultant pressure fluctuation in the plenum chamber about the mean was $< \pm 1.3\%$. The choice of mean velocity is somewhat arbitrary but was kept the same as in previous experiments for better comparison of results. It was also governed by the application to pneumatic rock drilling machinery for which such data were desired at the time. A further motivation was to consider a flow regime for which similar data were not already available so that existing knowledge could be extended.

Velocity field measurements were performed with a TSI 4-W argon-ion laser Doppler anemometer (LDA). The system was configured to use three beams operating with the green line with polarization to achieve two component velocity measurements. Bragg cell frequency shifting was used. Due to the high peak velocities in a cycle, a 40 MHz frequency shift was required for each velocity component in order to provide an adequate velocity range and avoid fringe bias associated

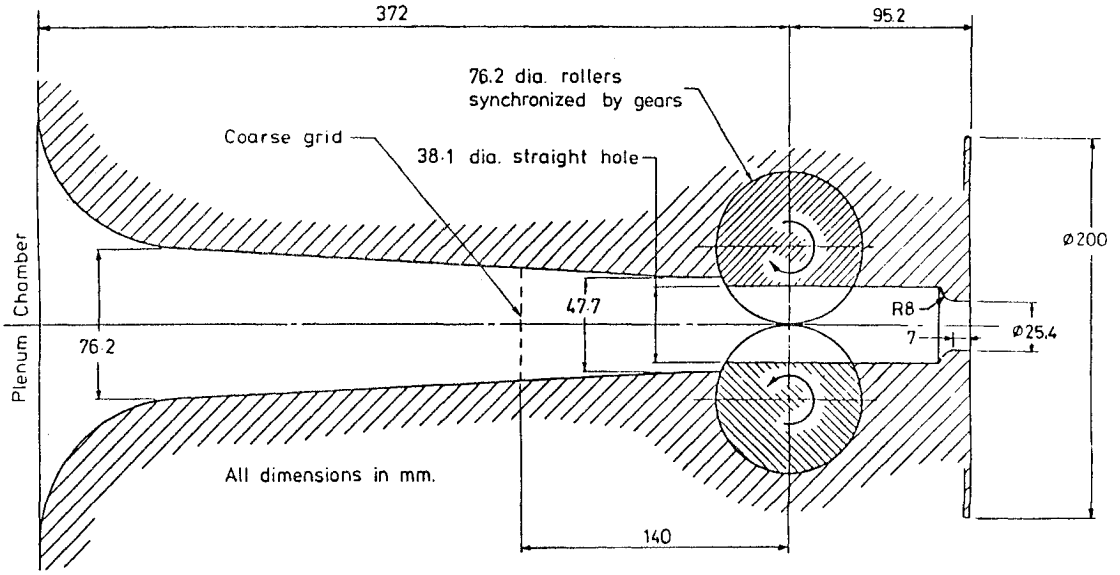

Fig. 1 Pulsating valve and exit geometry.

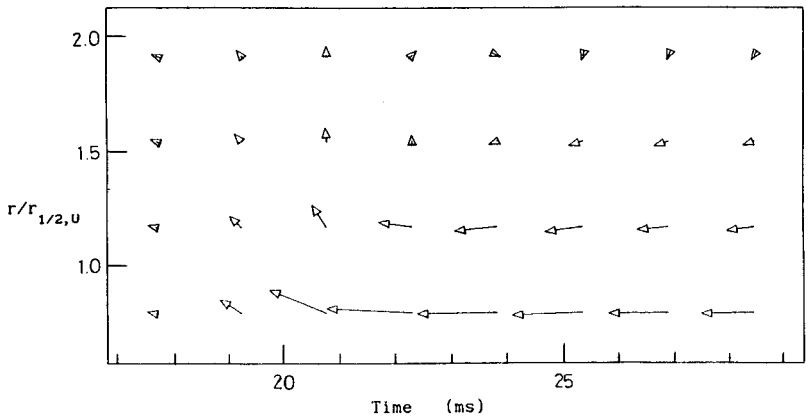

Fig. 2 Vector plot of starting vortex at $x/d = 20$: vectors scaled by maximum velocity in region, pulse period 100 ms.

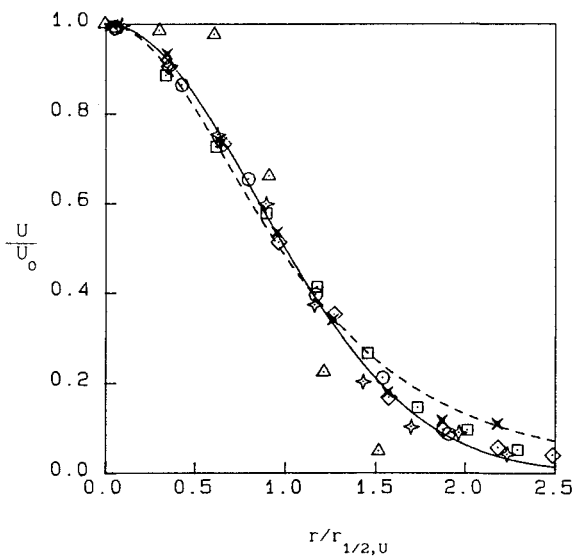

Fig. 3 Mean axial velocity profile, x/d: △ 1; □ 10; ○ 20; <> 30; + 40, × 50; ——— $U/U_0 = \exp[-\ell n 2(r/r_{1/2,U})^2]$; – – – $U/U_0 = [1 + 0.44(r/r_{1/2,U})^2]^{-2}$ (Ref. 6).

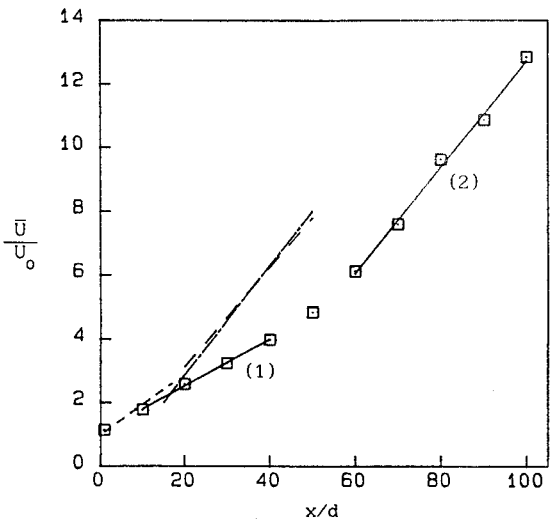

Fig. 4 Axial decay of centerline velocity: □ measured points; ——— (1) Eq. (5b) with $A_1 = 13.7$, $x_{01}/d = 14.7$; ——— Eq. (5b) with $A_1 = 6.0$, $x_{01}/d = -23.7$; – – – – Bremhorst and Harch[6]; —·— Wygnanski and Fiedler[17]; ———Rajaratnam.[18]

with the very short measuring volume transit times of a seed particle, especially in the near exit region.

Signal processing was by means of two TSI Model 1990A counter processors interfaced to a digital computer. Only coincident samples were used for covariance measurements, but all valid samples from the signal processors were used for single component results. Processor settings were for 1% comparison accuracy with 16 or 32 cycles per sample and signal validation on a 1 : 2 basis. Preliminary measurements indicated unsatisfactory results for fewer cycles per sample and excessive rejection for more cycles. Sample-hold weighting was used in order to minimize velocity bias.

Accuracy determination of LDA data is a particularly difficult topic. Two aspects need to be considered. The first is the repeatability of data and the second is absolute value determination. The first is influenced mainly by the fluctuating nature of the signal and reproducibility of experimental conditions. Mean velocity measurements were repeatable to ± 0.2 m/s. Turbulence data could be reproduced within the scatter obvious from the diagrams given. Absolute value determination is now known to be affected predominantly by the ratio of the measurement time scale relative to the flow time scale.[14] Unfortunately, the issue of which time is relevant remains to be resolved[15,16]; for a pulsed jet, this is complicated by the presence of multiple time scales. Consequently, it would be unwise to show absolute error limits for LDA measurements in case they are taken too literally.

Experimental Results

Mean Velocities

An appreciation of the velocity field can be obtained from phase-averaged velocity vector plots obtained at various distances from the jet exit. At the jet exit, pulses are short but elongate with distance downstream. Complete merging of the pulses does not result even at $x/d = 50$. At larger x/d, pulse merging is observed, which in the limit will lead to a steady jet. Radial spread characteristics are also readily visible. Of particular interest is the leading edge of the pulse where formation of a starting vortex, which is evident up to $x/d = 40$, can be seen (Fig. 2). Associated with this vortex is a radial outflow that covers a mere 3% of the on time of the jet. Reverse flow of small velocity magnitude can be identified, thus closing the starting vortex, the overall axial dimension of which at $x/d = 20$ is only 9% of the on time. From the vector plots it can be tentatively concluded that the pulse leading edge or starting vortex acts like a radial jet that will lead to a large transfer of high-momentum fluid out of the jet, whereas the diffuse return flow ensures that predominantly low-momentum will be entrained. Combination of these two effects should ensure a high total Reynolds stress and, hence, increased mixing.

Radial distributions of mean velocity are shown in Fig. 3 and compared with hot-wire anemometer results obtained by Bremhorst and Harch.[6] It is seen that the present measurements follow the traditional exponential distribution. The reason for the difference between LDA and hot-wire

anemometer measurements is that the latter results could not be corrected for any mean radial inflow velocity, reverse flow, and turbulence components. The near top-hat profile at $x/d = 1$ is consistent with expectations near an exit from a plenum chamber. Corresponding centerline velocity decay is given in Fig. 4; jet growth, represented by the half value radius $r_{1/2,U}$ (the point where the mean velocity is half that at the centerline), is given in Fig. 5. Particularly striking is the much slower decay of the centerline velocity U_0 up to $x/d = 50$ than is the case for steady jets.

Equations (5a–5c) are shown on Figs. 1–3, respectively. The A_1 and A_2 are constants, and x_{01} and x_{02} are effective origins.

$$\frac{U}{U_0} = \exp\left[-(\ell n 2)\left(\frac{r}{r_{1/2,U}}\right)^2\right] \tag{5a}$$

$$\frac{U_0}{\bar{U}} = A_1 \frac{d}{x + x_{01}} \tag{5b}$$

$$\frac{2r_{1/2,U}}{x + x_{02}} = A_2 \tag{5c}$$

From Fig. 4 it is seen that the near field has an effective origin well upstream of the exit. A consequent shift of x_{01} well downstream for the steady jet portion results in a considerable transition region. Also noteworthy is the linearity of U_0^{-1} in the pulse dominated region.

Volume Flow

Volume flow Q is defined by Eq. (6).

$$Q = \int_0^\infty 2\pi r U \, dr \tag{6}$$

Since the velocity distribution of Eq. (5a) is in excellent agreement with measurements, the analytical expression for volume flow, Eq. (7), can be applied. It should be noted that in this integration practically the total volume flow is contained within $3r_{1/2,U}$. Arbitrary termination of the tails of the velocity distribution is not necessary.

$$Q = \pi U_0 r_{1/2,U}^2 / \ell n 2 \tag{7}$$

Results of Fig. 6 again show the much larger volume flow than for steady jets. Entrainment, which is given by dQ/dx, is also much larger for the pulsed jet. The reduced level of volume flow compared with hot-wire results by Bremhorst and Harch[6] is due to the reduced mean velocity distribution tails at large radii.

Momentum Balance

In the absence of pressure gradients, jet momentum as expressed by Eq. (4) is constant. For the fully pulsed jet, Bremhorst and Harch[6] concluded from hot-wire anemometer measurements that the constancy of momentum does not apply for at least the first 10 exit diameters. Unfortunately, hot-wire measurement errors lead to uncertainty of the result due to a wire's response to several velocity components in a different manner to that required for momentum evaluation.

LDA measurements of the separate velocity terms allow direct calculation of momentum according to Eq. (4). A significant increase in momentum for the first 10 diameters from jet exit is still observed, as first reported by Bremhorst and Harch.[6] This is consistent with the presence of a negative pressure gradient acting to accelerate the fluid.

It is of interest to note that at $x/d = 10$, momentum carried by the mean motion [first component of momentum integral in Eq. (4)] is one third of that carried by the streamwise turbulence [second term in Eq. (4)]. At $x/d = 50$, on the other hand, momentum of the mean motion is 1.75 times that of the turbulence contribution. As can be seen with the aid of results from the next section, this is because most of the momentum associated with the turbulence term is in the periodic streamwise turbulence component, which dominates the flow at $x/d = 10$ but has decayed to almost negligible levels at $x/d = 50$. Thus, momentum increases due to the pressure effects in the first 10 diameters from the jet exit, and a significant transfer of momentum takes place from the periodic component to the mean flow in the first 50 diameters. The increase in momentum, as determined by Eq. (4) using LDA measurements of U and u, from jet exit to its fully developed value is 100%, which is much larger than the figure of 9% reported by Grinstein et al.[13] for steady and lightly pulsed jets.

Turbulence Intensities

The streamwise component of aggregate turbulence intensity, Fig. 7, shows a marked difference between a fully pulsed jet and steady jets due to the strong periodic component, whereas the radial and azimuthal component axial distributions are almost independent of x/d but occur at a higher level than for steady jets. From these results, it can be deduced that domination of the flow by the periodic component occurs up to $x/d = 50$. Separation of the intrinsic component representing shear generated turbulence, Fig. 7, shows

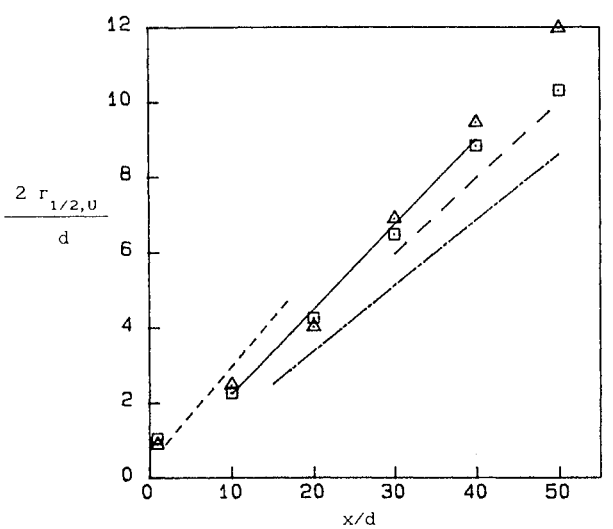

Fig. 5 Half value radius growth: □ vertical traverse; △ horizontal traverse; ——— Eq. (5c) with $A_2 = 0.225$, $x_{02}/d = -0.071$; - - - - Bremhorst and Harch[6]; —·— Wygnanski and Fiedler[17]; — — Rajaratnam.[18]

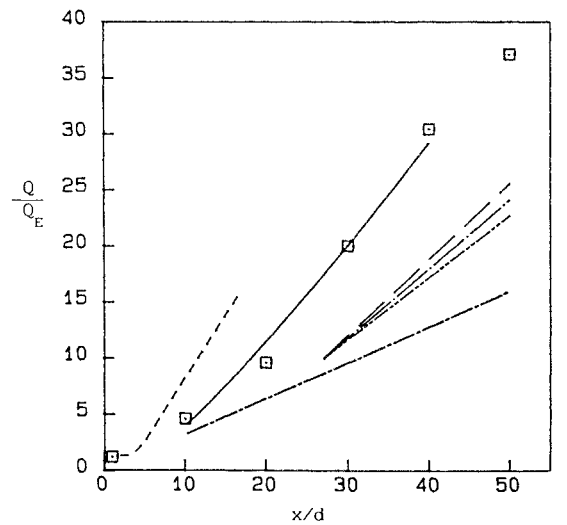

Fig. 6 Volume flow; □ integration of measured radial profiles at each x/d; ——— Eq. (7), for $10 \le x/d \le 40$; —·— steady jet of momentum M.[18,19] Slopes based on multiples of M for same mass flow as steady jet: - - - $\sqrt{3}\,M$; ———·——— 1.92 M; ———— 2.12 M; - - - - Bremhorst and Harch.[6]

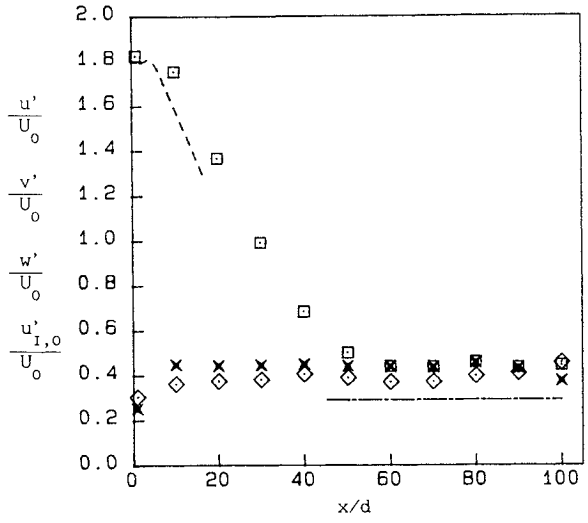

Fig. 7 Centerline turbulence intensities and intrinsic streamwise turbulence intensity (′ denotes rms value): □ u_0'/U_0; <> $v_0'/U_0 = w_0'/U_0$; × $u_{I,0}'/U_0$; ---- Bremhorst and Harch[6]; —·— Wygnanski and Fiedler[17]; —— Rajaratnam.[18]

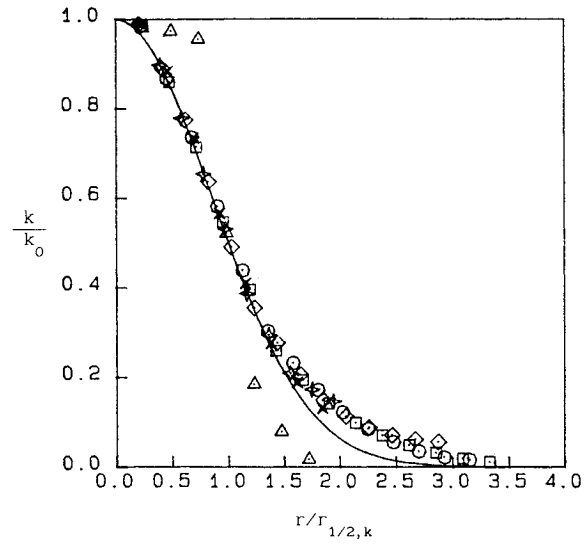

Fig. 8 Total turbulence energy profile; △ 1; □ 10; ○ 20; <> 30; + 40; × 50; ——— $\exp[-\ell n 2(r/r_{1/2,k})^2]$.

it to be essentially constant and at levels almost twice those of steady circular jets. Radial distributions of aggregate axial turbulence differ significantly from those in steady jets as the characteristic maxima in the shear layers are not visible.[6,20] This again is due to dominance of the pulsed component, but the intrinsic component displays the typical steady-jet distribution. Radial distributions of turbulence energy are given in Fig. 8 and are seen to follow the Gaussian distribution closely at $x/d \geq 10$. Near the jet exit a uniform distribution of turbulent kinetic energy is observed, which accounts for the deviation from the Gaussian profile.

Turbulent Shear Stress

Reynolds shear stress measurements were performed using instantaneous velocity data from the two channels. Values of u and v coincident within 96 μs (although most samples were within much less than this) were cross multiplied, weighted according to the sample-hold principle, summed, and averaged to give the final $\overline{uv}$ value. It should be noted that the data were weighted by the time to the next u or v sample, not the time to the next coincident sample. Since LDA measurements are sensitive to a large number of variables including the weighting method, measurements of Reynolds shear stress were performed in a steady jet and compared with values predicted from the mean velocity field. Excellent agreement was obtained between the two sets of results.

Reynolds shear stress measurements obtained in a pulsed jet, Fig. 9, are seen to follow trends similar to those in steady jets but are of much larger magnitude. The scatter is due to computer limitations, which did not permit longer averaging times. Hollis[20] has shown that the large increase in Reynolds shear stress is due to a significant contribution from the $\partial u^2/\partial x$ term in Eq. (2). The significance of the turbulence decay term exists up to $x/d \approx 50$, as seen from Fig. 7. The reason for this is that u^2 contains the pulsed as well as the intrinsic turbulence contributions.

Entrainment

Results of preceding sections have shown that the pulsed jet has both a higher entrainment and higher Reynolds shear stress than a steady jet of the same mass flow rate. Since Reynolds shear stress accounts for radial transport of mass, entrainment must be linked to it. The question, therefore, arises whether the pulsed jet has more entrainment than a steady jet when compared on a Reynolds shear stress or a jet momentum basis. This principle is contained in the entrainment equation, Eq. (8), given in Turner[11] for a steady jet with

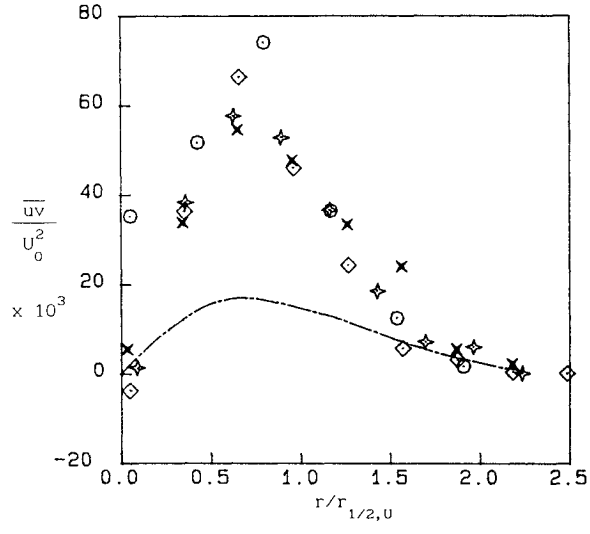

Fig. 9 Reynolds shear stress; △ 1; □ 10; ○ 20; <> 30; + 40; × 50; —·— steady jet.[17]

Gaussian velocity profiles under similarity conditions where M is the jet momentum for a given mean exit velocity and c_j is a constant:

$$\frac{dQ}{dx} = C_j M^{1/2} \tag{8}$$

where M for a steady jet is independent of x so that dQ/dx is proportional to $\bar{U}$, the jet exit velocity, assuming a top hat profile. If the pulsed jet is viewed as a quasisteady jet with a top-hat profile at exit both with radius and in time for an on-off period of 1 : 2, then the equivalent steady jet exit momentum is $3M$, which agrees with measurements. Its entrainment should, therefore, be $\sqrt{3}$ times that of a steady jet of the same mean velocity. As seen from Fig. 6, the corresponding slope that represents dQ/dx somewhat underestimates the measured entrainment.

Since pulsed jet exit momentum is increased by any pressure gradient effects, as already observed in connection with Eq. (3), a more appropriate comparison would, therefore, be with a momentum at a position in the flow where pressure effects are negligible but pulse domination of the flow still exists such as for $x/d > 10$. Measurements show this fully developed momentum to be 3.7–$4.5M$. An entrainment of

1.92–2.12 times that of a steady jet of the same mean exit velocity is, therefore, to be expected. The corresponding slopes in Fig. 6 show excellent agreement with this range of values, which is effectively based on local scaling.

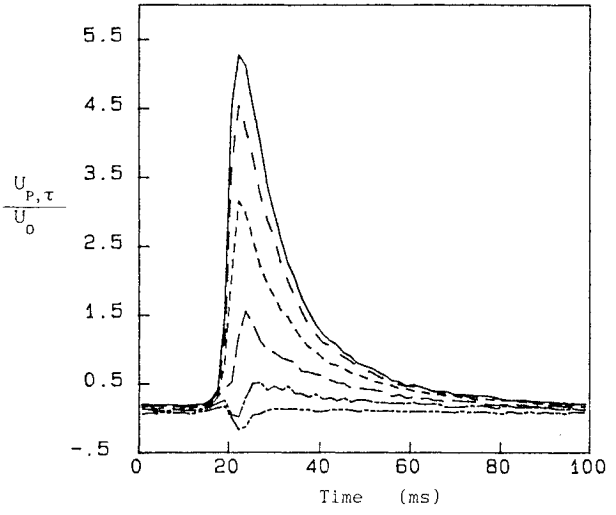

a) Axial periodic component

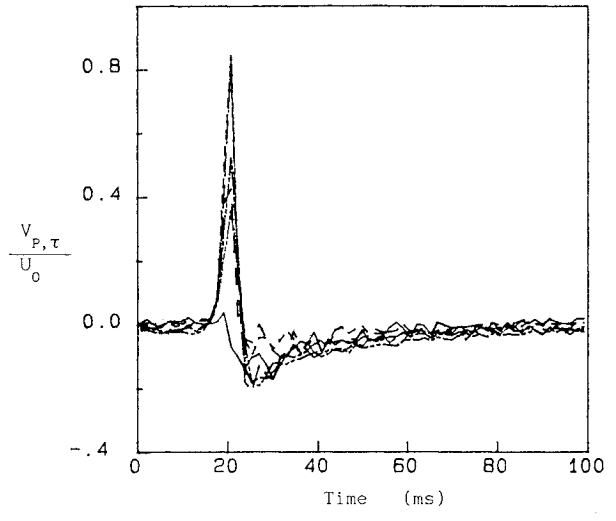

b) Radial periodic component

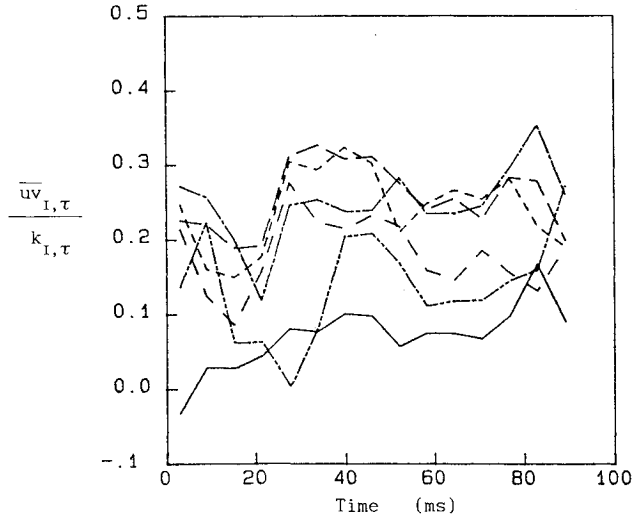

c) Shear stress to turbulent energy ratio

Fig. 10 Phase averaged results at $x/d = 20$: ——— $r/r_{1/2,U} = 0.06$; ——— 0.43; - - - - 0.80; ——— 1.17; —— 1.54; ——— 1.91.

Turner[11] has also given the entrainment equation based directly on Taylor's entrainment assumption, as in Eq. (9):

$$\frac{\partial}{\partial(x/d)}\left[\left(\frac{r_{1/2,U}}{d}\right)^2 \frac{U_0}{\bar{U}}\right] = 2\alpha\left(\frac{r_{1/2,U}}{d}\right)\frac{U_0}{\bar{U}} \tag{9}$$

where α has the experimentally determined value of 0.054 for steady jets. Data for the pulsed jet can be used together with Eq. (9) to show that α is in the range of 0.07–0.09 with the larger values being at smaller x/d. It is concluded, therefore, that the pulsed jet has characteristics in its developing region that increase the effective radial inflow velocity relative to U_0 above that applicable to a fully developed, steady jet.

Phase-Averaged Results

Pulse development and comparison with steady-jet behavior is better performed by means of phase averaging. A full set of such data is available in Hollis,[20] a sample being shown in Figs. 10a–10c. Figure 10a identifies the period during which significant flow takes place as well as a small reverse flow at the edge of the jet due to the starting vortex. The high-velocity outflow at the start of a pulse is seen to be followed by a very low-velocity inflow during the remainder of the pulse on time (Fig. 10b). Figures 10a and 10b quantify the vector plot data in Fig. 2. Intrinsic turbulence levels in the pulse dominated region, not shown here but available in Hollis,[20] vary continuously through the pulse at levels significantly above those of a fully developed steady jet. The ratio of intrinsic Reynolds stress to intrinsic turbulent kinetic energy throughout the pulse, Fig. 10c, does, however, fall within the narrow range of 0.2–0.3 for the bulk of the flow. This would suggest that any turbulence model based on stress scaling to provide closure of the flow equations should give satisfactory predictions.

Concluding Remarks

Data presented for a fully pulsed air jet with a significant no-flow period between pulses have given insight into a number of clearly identifiable flow characteristics. These divide the flow into regions associated with its development from the exit where the jet consists of a series of well-separated pulses to an almost steady jet far downstream. Particularly interesting is that such significant effects exist over a large spatial extent.

Momentum measurements show that a pressure gradient dominated region exists for the first 10 diameters from jet exit. Centerline mean velocity decay indicates a change in decay near $x/d = 50$ where decay upstream of this point is much slower than downstream with the latter being the same as for steady jets. Turbulence intensity measurements show the upstream region to be dominated by the periodic pulsation, which is reflected predominantly in the streamwise turbulence component, whereas the downstream region has characteristics similar to those of steady jets. This result is consistent with expectations but contradicts other published data, referred to earlier, that probably did not extend sufficiently far downstream to define the pulsed flow to steady-jet transition.

Volume flow results indicate much larger values than for steady jets with the axial gradient, which represents entrainment, being over twice that for steady jets. As this is of interest for mixing processes, it would be useful to know which feature of the flow gives rise to the increase. Results obtained have shown that the leading edge of a pulse acts like a radial jet that, with the associated return flow generated by a leading edge vortex, produces a higher Reynolds shear stress. In addition, it was found that the much higher Reynolds stress of the pulsed jet is associated with the axial decay of turbulent energy—a component found to be negligibly small in steady jets. The net effect of these two differences is, however, still adequately described by Taylor's entrainment hypothesis, which suggests that entrainment is proportional to

the square root of jet momentum provided that scaling is on the basis of fully developed jet momentum, that is, the value obtained in regions of negligible pressure gradient effects.

The practical significance of the preceding results is that jet entrainment for a given mass flow and given jet length can be increased significantly by pulsing with a no-flow period between pulses. Since results are still in general agreement with Taylor's entrainment hypothesis, the logical conclusion is that maximum entrainment for a given mass flow will be obtained for the method of pulsing that leads to maximum jet momentum and, hence, shear stress. The method investigated here appears to achieve higher entrainment than most others reported so far.

Acknowledgments

The authors are grateful for the significant financial support of the Australian Research Grants Scheme for purchase of the laser Doppler anemometer.

References

[1]Crow, S. C., and Champagne, F. H., "Orderly Structure in Jet Turbulence," *Journal Fluid Mechanics*, Vol. 48, Part 3, 1971, pp. 547–591.

[2]Binder G., Favre-Marinet, M., Kueny, J. L., Craya, A., and Laty, R., "Jets Instationnaires," *Labor de Mécanique des Fluides*, Université de Grenoble, Oct. 1971.

[3]Sarohia, V., Bernal, L., and Bui, T., "Entrainment and Thrust Augmentation in Pulsatile Ejector Flows," Jet Propulsion Lab., California Institute of Technology, Pasadena, CA, Publication 81-36, Aug. 1981.

[4]Bernal, L., and Sarhoia, V., "Experimental Investigation of Thrust Augmenting Ejector Flows," *Proceedings: Ejector Workshop for Aerospace Application*, edited by R. P. Braden, K. S. Nagaraja and H. J. P. von Ohain, AFAWL-TR-82-3059, 1982, pp. 551–570.

[5]McCroskey, W. J., "Some Current Research in Unsteady Fluid Dynamics," *Journal of Fluids Engineering*, Vol. 99, No. 1, 1977, pp. 8–38.

[6]Bremhorst, K., and Harch, W. H., "Near Field Velocity Measurements in a Fully Pulsed Subsonic Air Jet," *Turbulent Shear Flows I*, edited by F. Durst, B. E. Launder, F. W. Schmidt, and J. H., Whitelaw, Springer-Verlag, Berlin, 1979.

[7]Bremhorst, K., "Unsteady Subsonic Turbulent Jets," *Recent Developments in Theoretical and Experimental Fluid Mechanics*, edited by U. Müller, K. G. Roesner and B. Schmidt, Springer-Verlag, Berlin, 1979.

[8]Platzer, M. F., Simmons, J. M., and Bremhorst, K., "Entrainment Characteristics of Unsteady Subsonic Jets," *AIAA Journal*, Vol. 16, No. 3, 1978, pp. 282–284.

[9]Bremhorst, K., and Watson, R. D., "Velocity Field and Entrainment of a Pulsed Core Jet," *Journal of Fluids Engineering*, Vol. 103, No. 4, 1981, pp. 605–608.

[10]Kato, S. M., Groenewegen, B. C., and Breidental, R. E., "Turbulent Mixing in Nonsteady Jets," *AIAA Journal*, Vol. 25, No. 1, 1987, pp. 165–168.

[11]Turner, J. S., "Turbulent Entrainment: The Development of the Entrainment Assumption, and Its Application to Geophysical Flows," *Journal of Fluid Mechanics*, Vol. 173, Dec. 1986, pp. 431–471.

[12]Telford, J. W., "The Convective Mechanism in Clear Air," *Journal of the Atmospheric Sciences*, Vol. 23, No. 6, 1966, pp. 652–666.

[13]Grinstein, F. F., Oran, E. S., Boris, J. P., and Hussain, A. K. M. F., "Numerical Study of the Mean Static Pressure Field of an Axisymmetric Free Jet," *Preprints for the Tenth Symposium on Turbulence*, Univ. of Missouri-Rolla, Sept., 1986, pp. 16.1–16.23.

[14]Edwards, R. V., and Jensen, A. S., "Particle Sampling Statistics in Laser Anemometers: Sample and Hold Systems and Saturable Systems," *Journal of Fluid Mechanics*, Vol. 133, Aug. 1983, pp. 397–411.

[15]Winter, A. R., Graham, L. J. W., and Bremhorst, K., "Relationship Between Laser Doppler Anemometer Velocity Bias and Flow Time Scales," *Proceedings of the Tenth Australasian Fluid Mechanics Conference*, edited by A. E. Perry, Research Publications, Melbourne, Dec., 1989, pp. 1.29–1.32.

[16]Erdmann, J. C., and Tropea, C., "Statistical Bias of the Velocity Distribution Function in Laser Anemometry," *Laser Anemometry in Fluid Mechanics*, edited by R. J. Adrian, D. F. G. Durao, F. Durst, H. Mishina, and J. H. Whitelaw, Ladoan, Lisbon, 1984.

[17]Wygnanski, I., and Fiedler, H., "Some Measurements in the Self-Preserving Jet," *Journal of Fluid Mechanics*, Vol. 38, Part 2, 1969, pp. 577–612.

[18]Rajaratnam, N., *Turbulent Jets*, Elsevier, Amsterdam, 1976.

[19]Ricou, F. P., and Spalding, D. B., "Measurements of Entrainment by Axisymmetrical Turbulent Jets," *Journal of Fluid Mechanics*, Vol. 11, Part 1, 1961, pp. 21–32.

[20]Hollis, P. G., "Velocity Field Investigation of a Fully Pulsed Air Jet with a Laser Doppler Anemometer," Ph.D. Dissertation, University of Queensland, St. Lucia, Queensland, Australia, 1988.